# Electron-Vibration Interaction in the Presence of a Switchable Kondo Resonance Realized in a Molecular Junction

D. Rakhmilevitch,[1] R. Korytár,[2] A. Bagrets,[2,3] F. Evers,[2,4] and O. Tal[1]
[1]*Department of Chemical Physics, Weizmann Institute of Science, Rehovot 761001, Israel*
[2]*Institute of Nanotechnology, Karlsruhe Institute of Technology, Karlsruhe 76128, Germany*
[3]*Steinbuch Centre for Computing, Karlsruhe Institute of Technology, Karlsruhe 76128, Germany*
[4]*Institut Für Theorie der Kondensierten Materie, Karlsruhe Institute of Technology, Karlsruhe 76128, Germany*
(Received 22 June 2014; published 5 December 2014)

The interaction of individual electrons with vibrations has been extensively studied. However, the nature of electron-vibration interaction in the presence of many-body electron correlations such as a Kondo state has not been fully investigated. Here, we present transport measurements on a Copper-phthalocyanine molecule, suspended between two silver electrodes in a break-junction setup. Our measurements reveal both zero bias and satellite conductance peaks, which are identified as Kondo resonances with a similar Kondo temperature. The relation of the satellite peaks to electron-vibration interaction is corroborated using several independent spectroscopic indications, as well as *ab initio* calculations. Further analysis reveals that the contribution of vibration-induced inelastic current is significant in the presence of a Kondo resonance.

DOI: 10.1103/PhysRevLett.113.236603 PACS numbers: 72.15.Qm, 73.23.-b, 81.07.Nb, 85.65.+h

The Kondo effect is one of the most intensely studied many body phenomena, both experimentally and theoretically [1,2]. Although the basic Kondo exchange process was initially described in the 1960s and 1970s [3–6], new fascinating aspects are emerging to this day, including the orbital Kondo effect [7,8], the influence of Ruderman-Kittel-Kasuya-Yosida (RKKY) interactions [9,10], and the interplay between Kondo physics and superconductivity [11]. The Kondo effect has also been observed in molecular junctions, in which a molecule is located between two metallic electrodes [12–15]. In this system the localized magnetic moment on the molecule is screened by an exchange process with the itinerant electrons of the electrodes. This process leads to an enhanced density of states at the Fermi energy due to the emergence of the Abrikosov-Suhl resonance, observed in differential conductance measurements as a peak at zero-bias voltage. With the aid of molecular junctions, intriguing aspects of Kondo physics were explored such as the underscreened Kondo effect [16,17], the distribution of Kondo screening over different submolecular segments [18], and the influence of nearby molecules [19].

One of the attractive features of single-molecule junctions is the ability to couple molecular vibrations to conduction electrons [20]. In this context, molecular junctions are a natural platform for studying electromechanical interactions in the quantum regime. When an applied voltage across a molecular junction exceeds the energy of a given mode of vibration, this mode can be excited by the injected electrons. For a weak electron-vibration interaction in the off-resonance regime, an electron can scatter forward by exciting a vibration mode, resulting in an additional contribution to the current. Experimentally, this inelastic contribution manifests as a stepwise increase in the measured differential conductance at a voltage equivalent to the vibration energy [21]. This spectroscopic feature is commonly used to indicate the presence of a molecule in the junction as well as to chemically identify the molecule [22,23].

While a large body of experimental and theoretical findings addressing the interaction between independent electrons and vibrations is available, the understanding of electron-vibration interaction in correlated-electron systems has remained limited. Previously reported experiments detected a zero-bias Kondo peak in the differential conductance accompanied by satellite peaks at finite bias [24–26]. These features were often ascribed to the vibration assisted Kondo resonance for which the excess energy of the electrons due to a finite voltage is compensated by activating a vibration mode. However, establishing an explicit relation between vibrations and the Kondo effect remains an elusive challenge and the properties of electron-vibration interaction in the presence of such a many-body electron state were not addressed experimentally despite many theoretical studies [27–29].

In this Letter, we use molecular junctions based on silver (Ag) electrodes and copper-phthalocyanine (CuPc) molecules to identify the spectroscopic signature of electron-vibration interaction in the presence of a Kondo effect. This is confirmed by the evolution of satellite peaks to vibration-induced conductance steps when the Kondo resonance is suppressed. Furthermore, the nonmonotonic response of the satellite peaks to junction elongation reveals a typical signature of a vibration mode, as verified

 

by calculations. We find (i) a dominant influence of the Kondo effect on the evolution of the satellite peaks as a function of temperature and (ii) a substantial conductance contribution due to the vibration assisted Kondo effect with respect to the conductance of the zero-bias Kondo resonance.

The studied molecular junctions were fabricated in a mechanically controllable break-junction (MCBJ) setup [30] allowing a stable, subatomic control over the distance between the electrodes. Such changes were used before to modify both the manifestation of Kondo physics [25] and the activation of vibrations in atomic scale junctions [23,31,32]. The break junction samples were made of a silver wire segment (99.997%, GoodFellow), partially cut in the middle and attached to a flexible substrate. The samples were mounted into a vacuum chamber that was pumped and cooled to cryogenic temperature. The weak spot in the center of the wire was broken in cryogenic vacuum to expose ultraclean electrode apices. The bare silver atomic junction was characterized by recording conductance vs junction elongation for thousands of repeatedly formed contacts (see Supplemental Material [33]) and inelastic spectroscopy measurements [Fig. 1(a), blue]. CuPc molecules (99.95%, Sigma-Aldrich, further purified *in situ*) were introduced to the contact by controlled sublimation from a local source. The formation of molecular junctions was monitored by detecting conductance values below $\sim 1 G_0$, the typical conductance of a bare silver atomic contact, and verified using inelastic spectroscopy to detect molecular vibrations in bias voltages above the phonon spectrum of the metal [47].

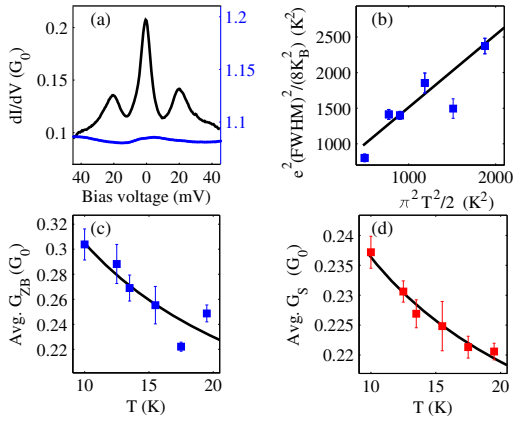


FIG. 1 (color online). (a) Typical differential conductance spectrum obtained before (blue) and after (black) admission of CuPc molecules to the silver atomic junction. (b) Full width at half maximum (FWHM) of the zero-bias peak as a function of temperature. The curve is a fit to Eq. (2). (c) Average conductance of the zero-bias peak ($G_{\mathrm{ZB}}$) as a function of temperature. The curve is a fit to Eq. (1). (d) Average conductance of the satellite peaks ($G_S$) as a function of temperature. The curve is a fit to Eq. (1) combined with an offset due to the background conductance of the zero-bias peak. Error bars indicate the standard error of the data set obtained on an ensemble of junctions at each temperature.

After admission of molecules into the junction, a prominent zero-bias peak was observed in 30% of the independently formed junctions, in most cases accompanied by two satellite peaks at finite bias [Fig. 1(a), black]. Since CuPc is known to have a spin 1/2 both in the gas phase as well as in epitaxial layers [48], and Kondo resonance was observed for CuPc adsorbed on a silver substrate in STM experiments [49], the Kondo effect is a possible source for the observed peak at zero bias. In order to test this possibility, we collected differential conductance spectra of 186 independently formed junctions measured at different temperatures and magnetic fields. The average conductance at zero bias and the full width at half-maximum (FWHM) of the zero-bias peak follow the appropriate functional dependence with temperature for a spin 1/2 Kondo impurity [50,51]:

$$G(T, V = 0) = \frac{\alpha}{[1 + (\frac{T}{T_K})^2 (2^{\frac{1}{0.22}} - 1)]^{0.22}} \tag{1}$$

$$\frac{e^2}{8k_B^2}(\mathrm{FWHM})^2 = (\pi T)^2/2 + T_K^2 \tag{2}$$

with Kondo temperatures of $T_K = 21 \pm 5$ K and $T_K = 22 \pm 5$ K, respectively [see the fitting in Figs. 1(b) and 1(c)].

As shown in Fig. 2(a), application of an external magnetic field perpendicular to the junction axis results in a notable increase in the average FWHM of the zero-bias peak. While a clear peak splitting was not observed due to the high temperature, Fig. 2(b) shows that at a magnetic field of 8.5 T, the zero-bias peak can be fitted by the sum of two Lorentzian functions, each with a FWHM of 6 mV, which are separated by 3.14 mV as expected for single molecule junctions with spin 1/2 Kondo resonance [12]. The evolution of the zero-bias peak as a function of temperature and applied magnetic field indicates that spin 1/2 Kondo correlations are the source of the zero-bias peak.

The appearance of satellite peaks accompanying the zero-bias Kondo resonance suggests that the Kondo effect plays a dominant role in the formation of these features. To examine our hypothesis, we analyzed the influence of temperature on the properties of the satellite peaks. As can be seen in Fig. 1(d), the decrease in the conductance of the satellite peaks with increasing temperature is described remarkably well by Eq. (1). Based on this fitting, the extracted Kondo temperature for the satellite peaks is $25 \pm 5$ K, which is similar to the Kondo temperature obtained for the zero-bias peak. We note that this analysis excludes the mechanism of a vibration-induced two-level system as the origin of the finite bias peaks [52,53].

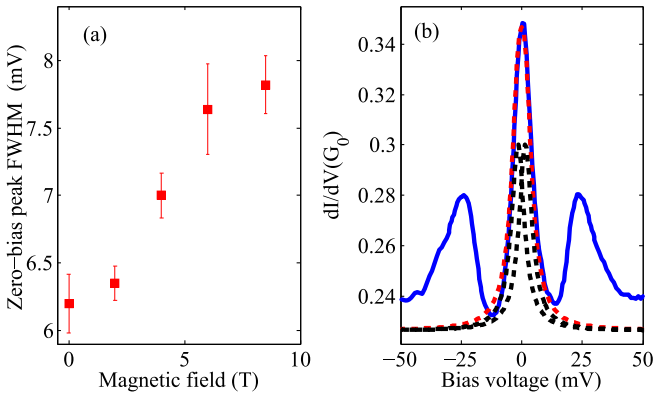


FIG. 2 (color online). (a) Dependence of the average zero-bias peak FWHM on external magnetic field. (b) Fitting of a zero-bias peak, obtained in an external magnetic field of 8.5 T, by the sum of two Lorentzians. Both the separation and the FWHM result from automatic fitting without any preset boundaries. The sum (dashed, red line) of the individual Lorentzians (dashed, black line) with a FWHM of 6 mV, separated by 3.14 mV, fits with the zero-bias peak with a FWHM of 8.5 mV.

In order to further study the origin of the satellite peaks, we focused on differential conductance spectra measured on an ensemble of independently formed molecular junctions. In 31 junctions, when the zero-bias peak was suppressed, as seen in Fig. 3(a), we observed conductance steps at voltage values corresponding to the satellite peaks [Fig. 3(b)]. Such an increase in the conductance as a function of voltage is a typical signature of vibration activation in the off-resonance conduction regime [21]. The presented vibration-induced conductance steps were observed for junctions with different conductance values, indicating that the excitation of the relevant vibration mode is not significantly susceptible to variations in the configuration of the junction. Moreover, evolution of conductance steps into satellite peaks at the same voltages was observed when the junctions were stretched [e.g., Fig. 3(c)], indicating a probable common origin for both features. This evolution can stem from conformational changes in the molecular junction as a result of stretching. Note that similar switching of a zero-bias Kondo effect due to conformational changes was previously observed both in STM [54] and MCBJ experiments [25,55].

To further establish the relation between the satellite peaks and molecular vibrations, we focus on the evolution of differential conductance spectra as a function of junction elongation. Figure 4(a) presents a subset of differential conductance curves for increasing interelectrode distances. As can be seen in Fig. 4(b), when the junction is stretched in steps of 0.25 Å the satellite peaks shift to higher voltage, up to a certain elongation. However, this tendency is inverted when the junction is stretched further; the satellite peaks are then shifted to lower voltage. Remarkably, a similar response to junction stretching can be expected for a vibration mode. Stretching the junction leads to enhancement of the vibration frequency in analogy to the increase of the pitch of a guitar string under tension [23]. This results in an increase of the onset voltage for vibration activation [57]. Further stretching eventually weakens the bonds between the molecule and the electrodes, leading to a

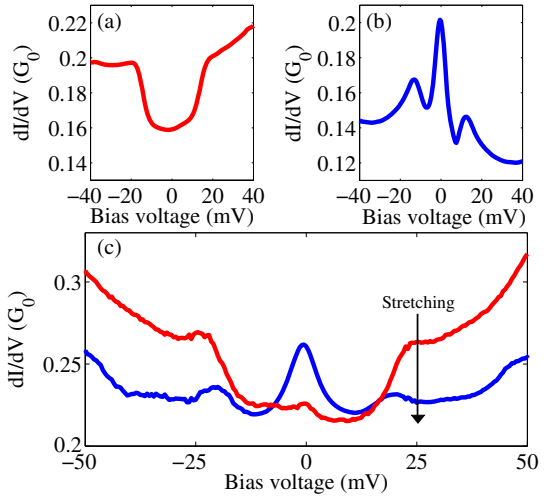


FIG. 3 (color online). Differential conductance curves vs applied voltage, measured on independently formed Ag/CuPc molecular junctions. (a) Finite-bias steps appear when the zero-bias peak is absent. (b) Finite-bias peaks appear only as satellites in the presence of a zero-bias peak. Note that the differential conductance curves exhibit some asymmetry, probably due to conductance fluctuations [56]. (c) Evolution of a differential conductance spectrum when the junction is stretched by 0.08 Å.

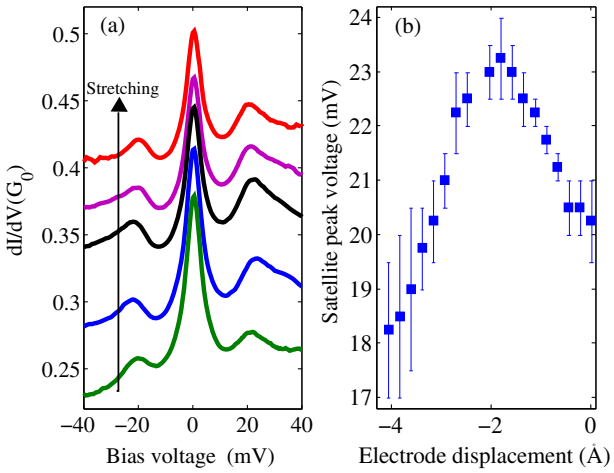


FIG. 4 (color online). (a) A sequence of differential-conductance curves taken at increasing interelectrode distances. The curves are shifted by $0.05G_0$. (b) Averaged voltage of the satellite peaks in each curve [exemplified in (a)] as a function of interelectrode separation. The data of the full stretching sequence is presented in (b), while (a) presents only some of the curves for better clarity. The error bars indicate deviations from the average.

decrease in the vibration energy and hence a decrease in onset voltage for vibration activation [23,31].

The structure of the junction and the corresponding vibration modes were analyzed using *ab initio* calculations. In the gas phase the CuPc molecule carries a spin 1/2 moment in a singly occupied orbital $b_{1g}$, localized near the copper center [58,59]. In contrast to the case of CuPc adsorbed on a Ag (100) surface [18], we find no significant charge transfer to the molecule, and the gas-phase electronic structure remains intact even after coupling to the electrode apices [33]. Hence, the experimental observation of the Kondo effect is expected. Out of the 20 candidate vibration modes in the relevant energy window of 10–35 meV, a specific mode was singled out based on (i) the study of vibration coupling to the $b_{1g}$ orbital in the gas-phase CuPc, and (ii) the analysis of stretching dependence of vibrations in the molecular junction. In essence, the $D_{4h}$ point group symmetry of the molecule implies a number of selection rules for the electron-phonon matrix elements of the $b_{1g}$ orbital. Consequently, out of all vibration modes in the relevant energy window, there is only one mode, $A_{1g}$, [see Fig. 5(a)], with energy of $\hbar\Omega_0 = 31$ meV and a sizable electron-phonon coupling $\lambda_0 = 6$ meV.

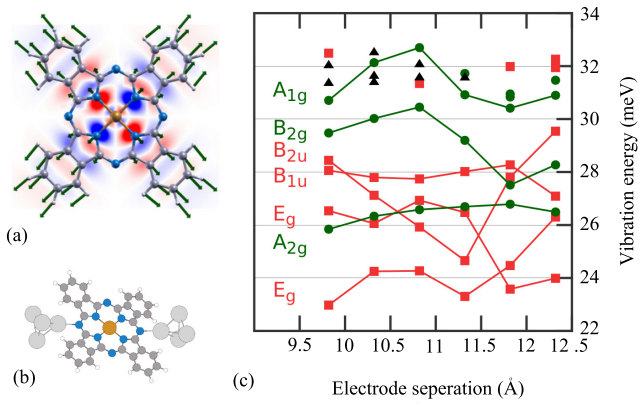


FIG. 5 (color online). Theoretical analysis of molecular vibrations. (a) Ball-and-stick model of CuPc (hydrogen is white, carbon is gray, nitrogen is blue, and copper is orange). In the background we show the $b_{1g}$ molecular orbital, that carries the Kondo-screened magnetic moment. Because of selection rules, only the $A_{1g}$ vibrational mode has a significant electron-phonon coupling matrix element; the atomic displacements (scaled by $\times 10$) of this eigenmode are shown with green arrows. (b) Ball-and-stick representation of the structure used to investigate the vibrations of CuPc in the junction (silver-large gray circles). (c) Flow of vibration frequencies of the junction presented in (b) at 6 successive elongations. The horizontal axis denotes the apex-to-apex distance. For vibrations with distinct character, the Mulliken symbol of the corresponding gas-phase CuPc mode is shown to the left. Modes with a markedly in-plane character are shown as green circles; modes with a markedly out-of-plane character are shown as red squares; modes without defined character are shown as black triangles.

To inspect the stretching dependence of vibration frequencies, we have considered the relaxed structure in Fig. 5(b), comprising the molecule bound to a pair of Ag pyramids [33]. In energetically favorable configurations the molecule binds to the Ag electrodes via the nitrogen atoms, restricting the possible orientations of the molecule in the junction. We have increased the apex-to-apex distance in successive steps and traced the behavior of vibrations, as presented in Fig. 5(c). Although the $D_{4h}$ symmetry is lifted, most of the junction modes retain their gas-phase character. Thus, stretching can be understood as an adiabatic flow of the vibration spectrum. The relevant mode, previously attributed to the gas phase $A_{1g}$, shows a nonmonotonic energy shift, of at least 2 meV, with a pronounced maximum, qualitatively reproducing the experimental observation. The vibration energy is approximately 10 meV higher as compared to the experimental data. We attribute this difference to (a) simplification in our electrode model, which lacks elasticity, and (b) to the more fundamental uncertainty of any density functional theory based estimation of atomic forces due to the approximate nature of the exchange-correlation functionals. For more information regarding the response of vibration modes with different symmetries to junction stretching, see [33].

To summarize up to this point, our analysis indicates that molecular vibrations coexisting with Kondo screening play a central role in the formation of the satellite peaks. The good agreement of Eq. (1) with our results suggests that within the experimental resolution, the participation of the vibration degree of freedom does not have a significant effect on the temperature dependence of the conductance at the satellite peaks. This weak dependence on temperature holds for $k_B T < 0.1\hbar\omega$ ($\hbar\omega \approx 20$ meV being the vibration mode energy), as was also shown for the amplitude of vibration-induced steps in the absence of Kondo screening [60,61].

Interestingly, we find that the inelastic conductance due to vibration activation is considerably large in the presence of Kondo screening. In the absence of the Kondo resonance, the fraction of inelastic conductance is approximately determined by the ratio between the height of the conductance step and the zero-bias conductance values [60,62]. Performing this analysis on curves exhibiting a step yields an average value of $13 \pm 1\%$, which is similar to previous observations in single molecule junctions [63]. For junctions exhibiting both zero-bias and satellite peaks, the ratio between the amplitudes of the two types of peaks provides the ratio of the inelastic vibration-assisted Kondo conductance with respect to the elastic Kondo conductance. By analyzing the ensemble of differential conductance curves exhibiting both peaks, we find this ratio to be $26 \pm 3\%$. This suggest that the electron-vibration interaction can be significant when Kondo screening emerges.

To conclude, we find clear indications for a vibration assisted Kondo effect in Ag/CuPc molecular junctions. The

presented study reveals the properties of electron-vibration interaction in a Kondo correlated electron system. In particular, we find a similar Kondo temperature for the zero-bias Kondo resonance and the vibration assisted Kondo process and a significant inelastic contribution to the Kondo conductance. We hope that our observations will stimulate further investigations, theoretical as well as experimental, of Kondo impurities that are coupled to bosonic baths.

We thank K. L. Narasimhan for his valuable help in developing a molecular evaporation source and M. Bürkle for discussions and sharing with us a development version of TURBOMOLE package, containing an EVIB module. O. T. thanks the Harold Perlman Family for their support and acknowledges funding by the Israel Science Foundation, the German-Israeli Foundation, the Minerva Foundation, the Gerhard Schmidt Minerva Center and the Yeda-Sela Center. A. B. acknowledges support of DFG through the research Grant No. BA 4265/2-1. Computational resources of the HC3 computer cluster at Steinbuch Centre for Computing (KIT) is acknowledged.

[1] A. C. Hewson, *The Kondo Problem to Heavy Fermions* (Cambridge University Press, Cambridge, England, 1997), ISBN 9780521599474.
[2] L. Kouwenhoven and L. Glazman, Phys. World **14**, 33 (2001).
[3] P. W. Anderson, Phys. Rev. **124**, 41 (1961).
[4] J. Kondo, Prog. Theor. Phys. **32**, 37 (1964).
[5] K. G. Wilson, Rev. Mod. Phys. **47**, 773 (1975).
[6] P. Nozières, J. Low Temp. Phys. **17**, 31 (1974).
[7] P. Jarillo-Herrero, J. Kong, H. S. J. Van Der Zant, C. Dekker, L. P. Kouwenhoven, and S. De Franceschi, Nature (London) **434**, 484 (2005).
[8] M.-S. Choi, R. López, and R. Aguado, Phys. Rev. Lett. **95**, 067204 (2005).
[9] Y.-S. Fu, Q.-K. Xue, and R. Wiesendanger, Phys. Rev. Lett. **108**, 087203 (2012).
[10] H. B. Heersche, Z. de Groot, J. A. Folk, L. P. Kouwenhoven, H. S. J. van der Zant, A. A. Houck, J. Labaziewicz, and I. L. Chuang, Phys. Rev. Lett. **96**, 017205 (2006).
[11] M. R. Buitelaar, T. Nussbaumer, and C. Schönenberger, Phys. Rev. Lett. **89**, 256801 (2002).
[12] J. Park, A. N. Pasupathy, J. I. Goldsmith, C. Chang, Y. Yaish, J. R. Petta, M. Rinkoski, J. P. Setna, H. D. Abruña, P. L. McEuen, and D. C. Ralph, Nature (London) **417**, 722 (2002).
[13] W. Liang, M. P. Shores, M. Bockrath, J. R. Long, and H. Park, Nature (London) **417**, 725 (2002).
[14] L. H. Yu and D. Natelson, Nano Lett. **4**, 79 (2004).
[15] S. Wagner, F. Kisslinger, S. Ballmann, F. Schramm, R. Chandrasekar, T. Bodenstein, O. Fuhr, D. Secker, K. Fink, M. Ruben, and H. B. Weber, Nat. Nanotechnol. **8**, 575 (2013).
[16] J. J. Parks, A. R. Champagne, T. A. Costi, W. W. Shum, A. N. Pasupathy, E. Neuscamman, S. Flores-Torres, P. S. Cornaglia, A. A. Aligia, C. A. Balseiro *et al.*, Science **328**, 1370 (2010).
[17] N. Roch, S. Florens, T. A. Costi, W. Wernsdorfer, and F. Balestro, Phys. Rev. Lett. **103**, 197202 (2009).
[18] A. Mugarza, C. Krull, R. Robles, S. Stepanow, G. Ceballos, and P. Gambardella, Nat. Commun. **2**, 490 (2011).
[19] V. Iancu, A. Deshpande, and S.-W. Hla, Phys. Rev. Lett. **97**, 266603 (2006).
[20] J. C. Cuevas and E. Scheer, *Molecular Electronics: An Introduction to Theory and Experiment*, World Scientific Series in Nanotechnology and Nanoscience (World Scientific, Singapore, 2010), ISBN 9789814282581.
[21] B. C. Stipe, M. A. Rezaei, and W. Ho, Science **280**, 1732 (1998).
[22] R. C. Jaklevic and J. Lambe, Phys. Rev. Lett. **17**, 1139 (1966).
[23] D. Djukic, K. S. Thygesen, C. Untiedt, R. H. M. Smit, K. W. Jacobsen, and J. M. van Ruitenbeek, Phys. Rev. B **71**, 161402 (2005).
[24] L. H. Yu, Z. K. Keane, J. W. Ciszek, L. Cheng, M. P. Stewart, J. M. Tour, and D. Natelson, Phys. Rev. Lett. **93**, 266802 (2004).
[25] J. J. Parks, A. R. Champagne, G. R. Hutchison, S. Flores-Torres, H. D. Abruña, and D. C. Ralph, Phys. Rev. Lett. **99**, 026601 (2007).
[26] I. Fernández-Torrente, K. J. Franke, and J. I. Pascual, Phys. Rev. Lett. **101**, 217203 (2008).
[27] R.-Q. Wang, Y.-Q. Zhou, and D. Y. Xing, J. Phys. Condens. Matter **20**, 045219 (2008).
[28] J. Paaske and K. Flensberg, Phys. Rev. Lett. **94**, 176801 (2005).
[29] J. König, H. Schoeller, and G. Schön, Phys. Rev. Lett. **76**, 1715 (1996).
[30] C. J. Muller, J. M. van Ruitenbeek, and L. J. de Jongh, Phys. Rev. Lett. **69**, 140 (1992).
[31] N. Agraït, C. Untiedt, G. Rubio-Bollinger, and S. Vieira, Phys. Rev. Lett. **88**, 216803 (2002).
[32] Y. Kim, H. Song, F. Strigl, H.-F. Pernau, T. Lee, and E. Scheer, Phys. Rev. Lett. **106**, 196804 (2011).
[33] See Supplemental Material at http://link.aps.org/supplemental/10.1103/PhysRevLett.113.236603,which includes Refs. [34–46].
[34] F. Pauly, J. K. Viljas, M. Bürkle, M. Dreher, P. Nielaba, and J. C. Cuevas, Phys. Rev. B **84**, 195420 (2011).
[35] R. Vardimon, M. Klionsky, and O. Tal, Phys. Rev. B **88**, 161404 (2013).
[36] V. Blum, R. Gehrke, F. Hanke, P. Havu, V. Havu, X. Ren, K. Reuter, and M. Scheffler, Comput. Phys. Commun. **180**, 2175 (2009).
[37] E. van Lenthe, E. J. Baerends, and J. G. Snijders, J. Chem. Phys. **101**, 9783 (1994).
[38] J. P. Perdew, K. Burke, and M. Ernzerhof, Phys. Rev. Lett. **78**, 1396 (1997).
[39] R. Korytár and N. Lorente, J. Phys. Condens. Matter **23**, 355009 (2011).
[40] R. Ahlrichs *et al.*, TURBOMOLE V6.6 (development version), program package for *ab initio* electronic structure calculations, Turbomole GmbH, www.turbomole.com (2014).
[41] A. Schäfer, H. Horn, and R. Ahlrichs, J. Chem. Phys. **97**, 2571 (1992).

[42] K. Eichkorn, O. Treutler, H. Öhm, M. Häser, and R. Ahlrichs, Chem. Phys. Lett. **240**, 283 (1995).
[43] P. Deglmann and F. Furche, J. Chem. Phys. **117**, 9535 (2002).
[44] P. Deglmann, F. Furche, and R. Ahlrichs, Chem. Phys. Lett. **362**, 511 (2002).
[45] P. Deglmann, K. May, F. Furche, and R. Ahlrichs, Chem. Phys. Lett. **384**, 103 (2004).
[46] M. Bürkle, J. K. Viljas, T. J. Hellmuth, E. Scheer, F. Weigend, G. Schön, and F. Pauly, Phys. Status Solidi B **250**, 2468 (2013).
[47] A. V. Khotkevich and I. K. Yanson, *Atlas of Point Contact Spectra of Electron-Phonon Interactions in Metals* (Kluwer Academic, Dordrecht, 1995), ISBN 9780792395263.
[48] J. E. Jiang, *Functional Phthalocyanine Molecular Materials* (Springer, Berlin, Heidelberg, 2010), ISBN 978-3-642-04751-0.
[49] A. Mugarza, R. Robles, C. Krull, R. Korytár, N. Lorente, and P. Gambardella, Phys. Rev. B **85**, 155437 (2012).
[50] D. Goldhaber-Gordon, J. Göres, M. A. Kastner, H. Shtrikman, D. Mahalu, and U. Meirav, Phys. Rev. Lett. **81**, 5225 (1998).
[51] K. Nagaoka, T. Jamneala, M. Grobis, and M. F. Crommie, Phys. Rev. Lett. **88**, 077205 (2002).
[52] W. H. A. Thijssen, D. Djukic, A. F. Otte, R. H. Bremmer, and J. M. van Ruitenbeek, Phys. Rev. Lett. **97**, 226806 (2006).
[53] A. Halbritter, P. Makk, S. Csonka, and G. Mihály, Phys. Rev. B **77**, 075402 (2008).
[54] A. Zhao, Q. Li, L. Chen, H. Xiang, W. Wang, S. Pan, B. Wang, X. Xiao, J. G. Hou, and Z. Qingshi, Science **309**, 1542 (2005).
[55] E. Scheer, T. Böhler, A. Edtbauer, S. Egle, M. Erbe, and T. Pietsch, J. Low Temp. Phys. **39**, 259 (2013).
[56] B. Ludoph and J. M. van Ruitenbeek, Phys. Rev. B **61**, 2273 (2000).
[57] T. Böhler, A. Edtbauer, and E. Scheer, New J. Phys. **11**, 013036 (2009).
[58] M.-S. Liao and S. Scheiner, J. Chem. Phys. **114**, 9780 (2001).
[59] N. Marom, O. Hod, G. E. Scuseria, and L. Kronik, J. Chem. Phys. **128**, 164107 (2008).
[60] M. Paulsson, T. Frederiksen, and M. Brandbyge, Phys. Rev. B **72**, 201101 (2005).
[61] L. J. Lauhon and W. Ho, Rev. Sci. Instrum. **72**, 216 (2001).
[62] This analysis holds for a single conduction channel as in the examined molecular junction, where the single *s* valence orbital of the silver atomic contact limits the number of conduction channels to 1. The presence of a single conduction channel was also verified by calculations.
[63] R. Ben-Zvi, R. Vardimon, T. Yelin, and O. Tal, ACS Nano **7**, 11 147 (2013).

# Electron-vibration interaction in the presence of a switchable Kondo resonance realized in a molecular junction
# Supplemental material

D. Rakhmilevitch,[1] R. Korytár,[2] A. Bagrets,[2,3] F. Evers,[2,4] and O. Tal[1]

[1]*Department of chemical physics, Weizmann institute of science, Rehovot, Israel*
[2]*Institute of Nanotechnology, Karlsruhe Institute of Technology, Karlsruhe, Germany*
[3]*Steinbuch Centre for Computing, Karlsruhe Institute of Technology, Karlsruhe, Germany*
[4]*Institut Fr Theorie der Kondensierten Materie, Karlsruhe Institute of Technology Karlsruhe, Germany*

(Dated: October 12, 2014)

PACS numbers: 81.07.Nb, 85.65.+h,73.23.-b

### Formation of Ag/CuPc molecular junctions

As a first step, the typical conductance as a function of junction elongation was analyzed for bare silver atomic junctions. The inset of Fig. S1(b) shows several conductance traces measured during breaking of a silver (Ag) wire prior to CuPc introduction. In order to sample a wide distribution of local junction geometries, the junction was deformed between measurements. This was performed by squeezing the contact until it exhibited a conductance of 70 $G_0$ before reopening the junction. The last conductance plateau before rupture is attributed to conductance through a cross section of a single atom with a typical conductance of around 1.0 $G_0$ [1, 2]. The most probable conductance is given by the main peak in Fig. S1(a) and the distribution of conductance as a function of junction elongation is presented by the histogram in Fig. S1(b). After CuPc molecules were introduced from a heated local source and the system was allowed to cool down, the histograms changed considerably. As can be seen in Fig. S1(c) and (d), new

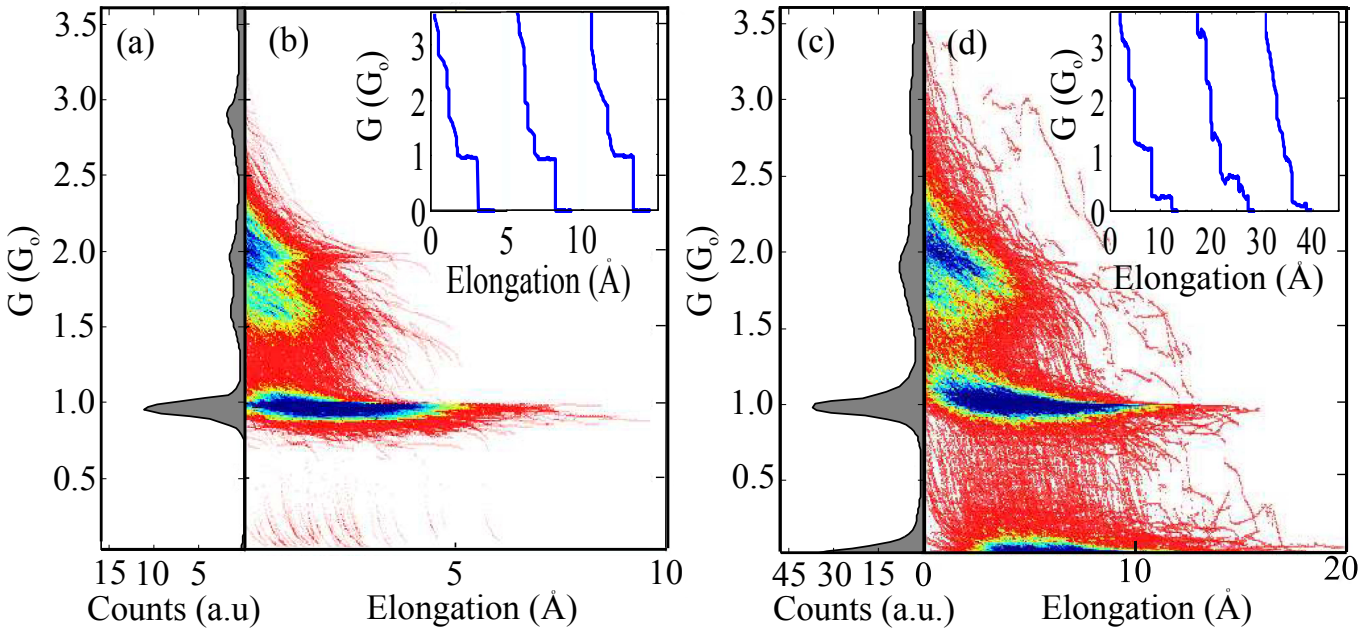


FIG. S1: (a,c) Conductance histograms that indicate the most probable conductance during junction elongation for bare Ag, and Ag/CuPc junctions, respectively. (b,d) 2D histograms of the number of counts at each conductance-elongation combination, zero displacement is set to a fixed conductance value of 2 $G_0$ for both junctions. Insets of (b) and (d): Examples for conductance traces as a function of junction elongation, shifted for clarity. The traces were measured for bare Ag and Ag/CuPc junctions, respectively. The measurements presented in this figure were taken at bias voltage of 50 mV and each histogram is constructed from 5,000 conductance traces.

conductance counts appear below 1.0 $G_0$, with significant contribution around 0.1 $G_0$. While Fig. S1(d) indicates that molecular junctions with higher conductance than 0.25 $G_0$ can be detected, clear zero-bias and satellite peaks were observed only for molecular junctions with off-resonance conductance below this value. The lower conductance values of the molecular junctions are also apparent when comparing individual traces (inset of Fig. S1(d)). In addition, the formation of molecular junctions was verified independently using inelastic electron spectroscopy, as described in the main text.

### Ab-initio calculations: Charge transfer

For the determination of optimal geometries and analysis of charge states we employed density functional theory (DFT) as implemented in the FHI-AIMS code [3]. Relativistic effects were included into the Kohn-Sham equations a posteriori by rescaling the Hamiltonian eigenvalues, according to the zeroth order regular approximation [4]. Electron-electron interactions were accounted for within the generalized gradient approximation and PBE exchange-correlation functional [5]. The basis set (termed tier1) contained 5 functions for hydrogen (angular momenta up to $l = 1$), 14 functions for carbon and nitrogen (up to $l = 2$) and 31 functions for each copper atom (up to $l = 3$). This basis set is equivalent to "double-$\zeta$ plus polarization" sets of quantum chemistry; for more details see Ref. [3]. Geometry optimization was performed in the framework of a closed-shell Kohn-Sham theory using 11-atom Ag clusters as electrodes; all electrode atoms were kept fixed. The geometry was considered relaxed if the largest residual force dropped below 0.01eV/Å. Self-consistency loop was terminated only if the forces did not differ by more than $10^{-4}$ eV/Å.

Firstly, we determined the relevant binding of the molecule to the Ag electrode. To this end, we used pairs of Ag clusters of pyramidal shape, each of 11 atoms, kept at a constant distance. As an initial guess for the geometry optimization, we placed the molecule between the pyramids at random orientations and positions. The Ag atoms were fixed and we optimized the positions of all the atoms of the CuPc molecule. We have found that in most cases the molecule binds to the apex via one of the four outward nitrogens (an example is shown in the inset of Fig. S2). Only when this Ag-N bond was not possible due to geometry constraints, we found an Ag-C bond. We inspected the charge state by using six different relaxed configurations in a spin-polarized DFT. We studied the charge state as a function of the electrode volume used in the simulation. Fig. S2 shows that with increasing electrode volume, a clear tendency towards a small charge injection of the order of -0.15 $|e|$ is observed. We have seen that most of the transferred charge goes to the ligands. In view of this result we conclude that the ligands can not develop a sizable magnetic moment and the spin moment originates mainly from the copper ion, as in the gas-phase CuPc. This is in

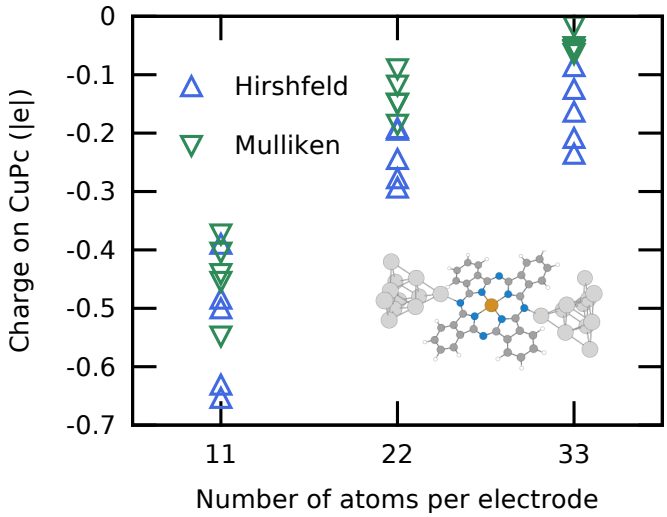


FIG. S2: Charge of CuPc contacted by Ag electrodes calculated by DFT. Negative values indicate electron excess. The horizontal axis shows the number of atoms per electrode. Mulliken and Hirshfeld charges are represented by different symbols. The plot includes results of six different relaxed structures (not distinguished graphically). In the bottom right corner there is an example of an optimized structure with 11 atoms per electrode.

stark contrast with CuPc adsorbed on the Ag(100) surface [6] with ligands developing an independent spin moment. Thus, our calculations predict that CuPc in a silver break-junction is a spin-half scattering center which is subjected to a Kondo effect.

### Electron-phonon coupling

In this section, we provide more details about the electron-phonon coupling calculation in the gas-phase CuPc. We have employed quantum chemistry package TURBOMOLE [7] to estimate the electron-phonon coupling constants of the "Kondo-active" $b_{1g}$ orbital to vibration modes of the CuPc molecule. Calculations were carried out using DFT within a generalized gradient approximation (PBE functional), contracted Gaussian-type basis sets of split-valence quality with polarization functions (def-SVP) [8] and corresponding Coulomb-fitting basis sets within the resolution of identity approximation [9]. The atomic structure of the molecule was relaxed assuming a planar geometry with a $D_{4h}$ symmetry. We obtained the vibration frequencies by solving an eigenvalue problem for a mass-weighted Hessian matrix, which was evaluated semi-analytically as outlined in Refs. [10–12].

Matrix elements $M^{\mu}_{nm}$ of the (second-quantized) electron-vibration interaction of the form $\sum_{\mu} M^{\mu}_{nm}(b^{\dagger}_{\mu}+b_{\mu})d^{\dagger}_{n}d_{m}$, involving vibration modes $\mu$ and a pair of Kohn-Sham (KS) molecular orbitals $m$ and $n$, were computed based on the first-order derivatives of the KS operator $H^{\mathrm{KS}}$ with respect to nuclear displacements $\delta\mathbf{R}_a$:

$$M^{\mu}_{nm} = \sum_{\mathbf{R}_a}^{\text{atoms}} \sqrt{\frac{\hbar}{2M(\mathbf{R}_a)\Omega_{\mu}}} \sum_{i=x,y,z} u^{i}_{\mu}(\mathbf{R}_a) \left\langle n \left| \frac{\partial H^{\mathrm{KS}}}{\partial(\delta R^{i}_{a})} \right| m \right\rangle .$$

Here $\mathbf{u}_{\mu}(\mathbf{R}_a)$ are normal modes (normalized eigenvectors of the mass-weighted Hessian matrix), $\Omega_{\mu}$ are the corresponding frequencies, and KS Hamiltonian $H^{\mathrm{KS}}$ comprises the electrostatic potential of ions and single-particle contributions due to kinetic energy, Hartree- and exchange-correlation terms (see Ref. [13] for further details). In a nutshell, the matrix element $M^{\mu}_{nm}$ is the energy cost for a shift of the atoms from their equilibrium positions by the elementary oscillator lengths, $\sqrt{\hbar/M(\mathbf{R}_a)\Omega_{\mu}}$, into the direction of the normal mode at hand. We are interested in the diagonal matrix elements $\lambda^{\mu} = M^{\mu}_{kk}$, where $k$ is a single-occupied orbital of $b_{1g}$ symmetry, involved in the formation of the Kondo resonance. We have found that due to the high symmetry of the molecule all coupling constants $\lambda^{\mu}$, except for a single one, are vanishing in the energy range below 50 meV. The selected vibration mode with nonzero constant $\lambda_0$ has energy $\hbar\Omega_0 = 31$ meV. It is a "breathing" mode (Fig. S3) of $A_{1g}$ symmetry associated with the unitary representation of the $D_{4h}$ group. For the given mode, $\lambda_0 = 6$ meV that corresponds to a dimensionless coupling constant $g = (\lambda_0/\hbar\Omega_0)^2 \approx 0.04$. The selection rules for the $b_{1g}$ molecular orbital can be understood in simple terms: firstly, we note that the $b_{1g}$ has an important contribution from the $d_{x^2-y^2}$ orbital of copper [14]. Its on-site energy is controlled by the size of square planar splitting of the $d$ shell. If the atoms move following the $A_{1g}$ representation, the four nitrogens around the copper modulate the splitting (see green arrows in Fig. S3). On the other hand, if the $B_{2g}$ mode is realized instead, the on-site energy is unchanged to first order.

### Vibrations of the molecular junction

For the analysis of vibrations of CuPc within a molecular junction we used a pair of Ag clusters each of four atoms. The optimal geometries and vibration frequencies were calculated with help of FHI-AIMS package [3] using "strict" parameter settings. The numerical basis set of atom-centered orbitals (termed tier2) contained 15 functions for hydrogen, 39 for carbon and nitrogen, 40 for copper and 49 for Ag. During relaxation steps, all Ag atoms were kept at fixed positions while atoms of CuPc were able to relax their coordinates unless residual forces dropped below $10^{-4}$ eV/Å.

We prepared six geometries with increasing distance between the apex atoms (from 10.8 to 12.3Å) by displacing the electrodes in successive steps. This set of geometries covers a rather wide range of the junction conformations: as the separation between apex atoms increases, the molecule is either (i) tilted with respect to the junction axis, (ii) stretched within the junction, or (iii) the molecular junction is almost ruptured with the molecule being contacted primary to the one apex atom only. We calculate the vibration modes of the full structure by a finite-difference method (atomic displacement was 0.025Å; see a remark on this setting below). We assign an infinite mass to the atoms of Ag.

Figure 4 of the main text shows the vibration frequencies of the structure as a function of stretching. Although the symmetries of the gas-phase molecule are partially lifted, the majority of the vibrations bears good resemblance to

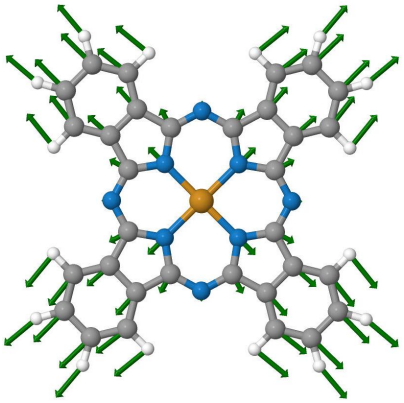

$A_{1g}$

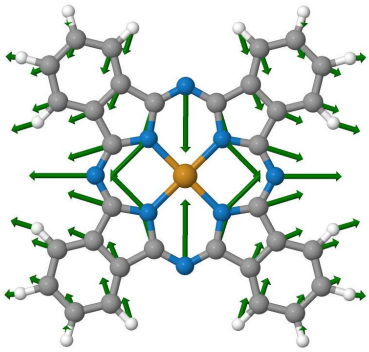

$B_{2g}$

FIG. S3: Vibrations of CuPc in the gas phase: the $A_{1g}$ and $B_{2g}$ modes. Nitrogen=blue, carbon=gray, hydrogen=white, copper=orange. The direction of motion of atoms is indicated by green arrows (rescaled by $\times 10$).

their parent vibrations of the molecule in the gas-phase. This allows us to trace each vibration mode as the distance between Ag clusters increases (i.e., junction is stretched). In all structures, we see a gap in the vibration spectrum, spanning the range 19 - 24 meV. Below the gap the vibrations react only weakly to stretching. The vibrations above the gap show a rich behavior: flat, monotonous and even non-monotonous. In the whole energy window considered, the vibrations of the two top-most connected lines have a pronounced maximum. They correspond to the $A_{1g}$ and $B_{2g}$ modes (shown in Fig. S3).

A few remarks on the interpretation of the calculated stretching dependence are in order. Firstly, we have verified the adequacy of the finite-difference approximation. For a single geometry, we have compared the frequencies obtained by two distinct sets of atomic displacements: 0.0025Å and 0.001Å. The absolute differences in frequencies inside the energy window 17 - 32 meV were lower than 0.1 meV. The second check concerned the electrode model. The data in Fig. 4 of the main text were calculated with Ag atoms being infinitely heavy; the electrode's dynamics was frozen. In reality, molecular modes couple to the continuum of electrode's phonon bands. Yet, most of the CuPc modes will remain localized due to differences in atomic masses and bond stiffness in the molecule and electrode's material. As a result of the electrode's elasticity the CuPc vibrations will (i) likely shift downwards in energy and (ii) perhaps flatten their stretching dependence. To inspect the second possibility, we have carried over calculations of the vibrations by allowing the apices to move (mass goes finite). We have observed that in most cases the apices admix very little to the molecular vibrations. The vibrations between 20 and 34 meV acquire a shift typically less then 1 meV. The frequency of the $A_{1g}$ mode retains the maximum and the relative height of the peak is 2 meV.

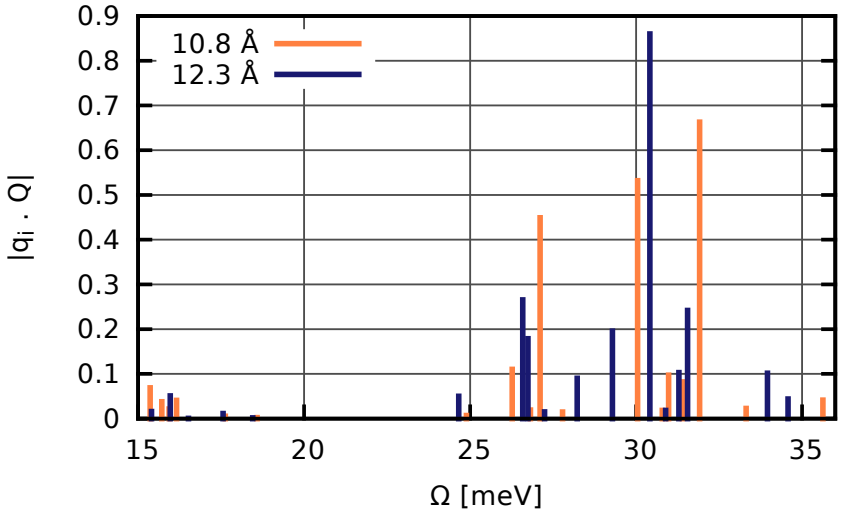


FIG. S4: Absolute values of the projection of junction's vibration eigenmode $q_i$ onto the $A_{1g}$ mode (with components $Q$) of the CuPc in the gas-phase. The $q_i$ vary on the horizontal axis and are labeled by their eigenenergy. For the junction vibration modes we chose two structures: at 10.8 and 12.3Å electrode separations.

### Stretching dependence of vibration modes

The vibration modes of atomic and molecular junctions based on individual atoms, atomic chains or diatomic molecules were classified in the past as longitudinal or transverse modes, describing motion along or perpendicular to the junction axis, respectively [15–17]. The symmetry of the vibration modes can be determined from the response of the onset energy of the vibration mode to an applied tension as a result of mechanical stretching of the junction. Longitudinal modes are characterized by a decrease in the vibration energy when stretching the junction. This response results from weakening of bonds between the molecule and the electrodes. Transverse modes, however, are characterized (at a certain stretching range) by an increase in the vibration energy in an analogy to a guitar string, followed by a decrease in vibration energy due to bond weakening.

### Projected vibration modes

In order to verify the intuitive picture of the eigenmode flow we have calculated numerically the projection of the vibration modes of the junction onto the gas-phase mode $A_{1g}$. The $A_{1g}$ mode is represented by a vector $Q$ with $3N$ components, where $N$ is the number of atoms in CuPc. $Q$ is obtained from the diagonalization of the mass-weighted Hessian matrix. Similarly, the junction modes are represented by vectors $q_i \quad i = 1, \ldots, 3N$ in a $3N$ dimensional space (note that there are no degrees of freedom associated with Ag). The projection is shown in Fig. S4, where the vibrations $q_i$ are labeled by their energy. We see that $A_{1g}$ is spread over several junction vibration modes. In the vicinity of the mode with maximum projection we find other modes with a significant $A_{1g}$ contribution. Taking into account a Kondo width in the order of $\approx 5$ meV we are lead to conclude that the fine structure of the junction modes will not be detectable experimentally.

[1] F. Pauly, J. K. Viljas, M. Bürkle, M. Dreher, P. Nielaba, and J. C. Cuevas, Physical Review B **84**, 195420 (2011).
[2] R. Vardimon, M. Klionsky, and O. Tal, Physical Review B **88**, 161404 (2013).
[3] V. Blum, R. Gehrke, F. Hanke, P. Havu, V. Havu, X. Ren, K. Reuter, and M. Scheffler, Computer Physics Communications **180**, 2175 (2009).
[4] E. van Lenthe, E. J. Baerends, and J. G. Snijders, The Journal of Chemical Physics **101**, 9783 (1994).
[5] J. P. Perdew, K. Burke, and M. Ernzerhof, Phys. Rev. Lett. **78**, 1396 (1997).
[6] R. Korytár and N. Lorente, Journal of Physics: Condensed Matter **23**, 355009 (2011).

[7] R. Ahlrichs and et al., *TURBOMOLE V6.6 (development version), program package for ab initio electronic structure calculations*, Turbomole GmbH, www.turbomole.com (2014).
[8] A. Schäfer, H. Horn, and R. Ahlrichs, The Journal of Chemical Physics **97**, 2571 (1992).
[9] K. Eichkorn, O. Treutler, H. Öhm, M. Häser, and R. Ahlrichs, Chemical physics letters **240**, 283 (1995).
[10] P. Deglmann and F. Furche, The Journal of chemical physics **117**, 9535 (2002).
[11] P. Deglmann, F. Furche, and R. Ahlrichs, Chemical physics letters **362**, 511 (2002).
[12] P. Deglmann, K. May, F. Furche, and R. Ahlrichs, Chemical physics letters **384**, 103 (2004).
[13] M. Bürkle, J. K. Viljas, T. J. Hellmuth, E. Scheer, F. Weigend, G. Schön, and F. Pauly, physica status solidi (b) **250**, 2468 (2013).
[14] M.-S. Liao and S. Scheiner, The Journal of Chemical Physics **114**, 9780 (2001).
[15] D. Djukic, K. S. Thygesen, C. Untiedt, R. H. M. Smit, K. W. Jacobsen, and J. M. van Ruitenbeek, Phys. Rev. B **71**, 161402 (2005).
[16] T. Böhler, A. Edtbauer, and E. Scheer, New J. Phys. **11**, 013036 (2009).
[17] N. Agraït, C. Untiedt, G. Rubio-Bollinger, and S. Vieira, Phys. Rev. Lett. **88**, 216803 (2002).